Growth model for plasma-assisted molecular beam epitaxy of N-polar and Ga-polar $In_xGa_{1-x}N$

Digbijoy N. Nath, Emre Gür, Steven A. Ringel, and Siddharth Rajan

Citation: Journal of Vacuum Science & Technology B **29**, 021206 (2011); doi: 10.1116/1.3562277
View online: https://doi.org/10.1116/1.3562277
View Table of Contents: https://avs.scitation.org/toc/jvb/29/2
Published by the American Vacuum Society

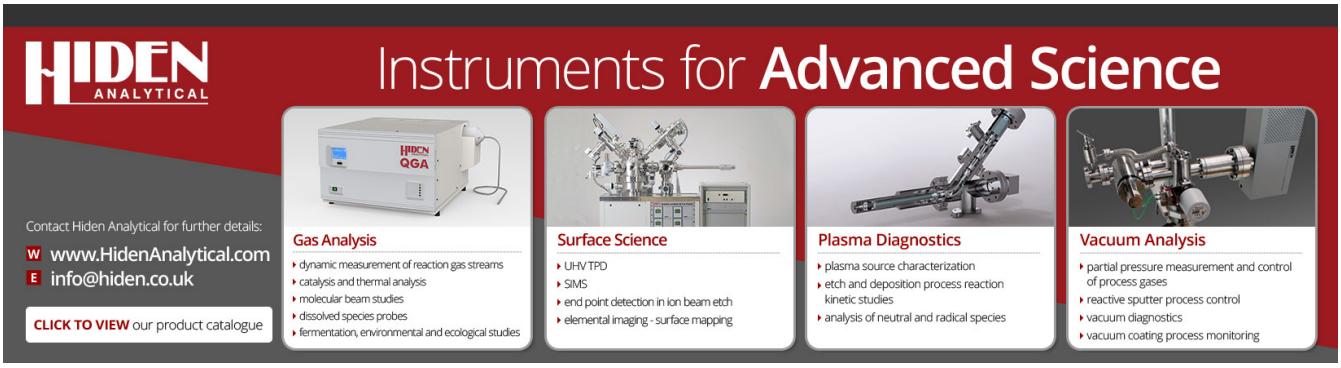

Growth model for plasma-assisted molecular beam epitaxy of N-polar and Ga-polar $In_xGa_{1-x}N$

Digbijoy N. Nath[a)]
Department of Electrical and Computer Engineering, The Ohio State University, Columbus, Ohio 43210

Emre Gür
Department of Electrical and Computer Engineering, The Ohio State University, Columbus, Ohio 43210 and Department of Physics, Faculty of Science, Atatürk University, 25240 Erzurum, Turkey

Steven A. Ringel and Siddharth Rajan
Department of Electrical and Computer Engineering, The Ohio State University, Columbus, Ohio 43210

(Received 27 August 2010; accepted 12 February 2011; published 10 March 2011)

The authors have developed a comprehensive model for the growth of N-polar and Ga-polar $In_xGa_{1-x}N$ by N_2 plasma-assisted molecular beam epitaxy. GaN films of both polarities were coloaded and $In_xGa_{1-x}N$ was grown in the composition range of $0.14<x<0.59$ at different growth temperatures keeping all other conditions identical. The compositions were estimated by triple-axis ω-2θ x-ray diffraction scans as well as by room temperature photoluminescence measurements. The dependence of the In composition x in $In_xGa_{1-x}N$ on growth temperature and the flux of incoming atomic species is explained using a comprehensive growth model which incorporates desorption of atomic fluxes as well as decomposition of InN component of $In_xGa_{1-x}N$. The model was found to be in good agreement with the experimental data for $In_xGa_{1-x}N$ of both polarities. A N-polar $In_{0.31}Ga_{0.69}N/In_{0.05}Ga_{0.95}N$ multi-quantum-well structure grown with conditions predicted by our growth model was found to match the compositions of the active layers well besides achieving a smooth surface morphology at the quantum-well/barrier interface. The understanding of growth kinetics presented here will guide the growth of $In_xGa_{1-x}N$ for various device applications in a wide range of growth conditions. © *2011 American Vacuum Society.* [DOI: 10.1116/1.3562277]

I. INTRODUCTION

The ternary $In_xGa_{1-x}N$ alloy system has been receiving wide attention especially for optoelectronic device applications such as blue/green lasers and light emitting diodes (LEDs). With its band gap (0.7–3.4 eV) spanning the entire visible and near infrared spectrum, $In_xGa_{1-x}N$ has also attracted interest for possible multijunction solar cells[1] since it encompasses almost the entire solar spectrum. Although $In_xGa_{1-x}N$ based blue diodes and white light sources are now commercially available, achieving emission in the green (~520 nm) and longer wavelength range with high efficiency and acceptable output power still poses severe challenges. It is difficult to grow high quality $In_xGa_{1-x}N$ with high In-mole fractions in the range of $0.25<x$ to achieve emissions in the longer wavelengths because the optimal growth conditions for the alloy components InN and GaN are significantly different. While a steady-state Ga metal bilayer coverage at optimal growth temperatures (~710 °C) enhances adatom diffusion leading to superior surface and material qualities for plasma-assisted molecular beam epitaxy (PAMBE) growth of GaN,[2] InN growth by MBE is limited to ~500 °C because of its inherent thermal instability and decomposition temperatures lower than that of desorption of metallic In.[3] This is significantly lower than optimal growth temperatures needed for the growth of GaN (~710 °C) which therefore deteriorates the quality of $In_xGa_{1-x}N$ films grown. More recently however, PAMBE grown Ga-polar InGaN based LEDs have been shown to exhibit output powers of 9 mW at 385–400 nm (Ref. 4) and 3 mW at 450 nm (Ref. 5) at injection currents of 1 and 0.1 A, respectively, which, however, are still far from achieving green or longer wavelength ranges.

Recently, the reversed direction of polarization of GaN, i.e., N-polar orientation, was explored to exploit the advantages for high-speed performance of highly scaled transistors.[6,7] It was also demonstrated that PAMBE growth of N-polar InN can be done at approximately 100 °C higher than the thermal dissociation limit of In-polar InN.[8–11] This implies that N-polar InGaN with higher In compositions can be grown at higher growth temperatures than In(Ga)-polar InGaN, and films with lower point defect incorporation and better optical properties may be expected. In addition, the reversed direction of polarization may have other advantages from the device design perspective. However, N-polar InGaN growth reports have been few so far[12,13] due to the challenges in the growth of high composition InGaN. This paper aims to provide a comprehensive understanding of In incorporation in N-polar InGaN as compared to Ga polar with a quantitative growth model that explains the variation of In-mole fraction in $In_xGa_{1-x}N$ with respect to the change in the growth temperatures. There have been reports published earlier modeling the MBE growth of $In_xGa_{1-x}N$,[14–16] but they were reported before the correct estimation of InN

a)Author to whom correspondence should be addressed; electronic mail: nathd@ece.osu.edu

band gap as ~0.7 eV. Thus, the model proposed here is more accurate in light of a revised InN band gap.

II. EXPERIMENTAL DETAILS AND UNDERLYING PHYSICS

Samples used in this study were grown by PAMBE in a Veeco Gen 930 system equipped with standard effusion cells for Ga and In. Active nitrogen was supplied using a Veeco rf plasma source. The substrates used were N-polar freestanding LED quality GaN templates (dislocation density of $\sim 10^8$ cm^{-2}) obtained from Lumilog and Ga-polar GaN on sapphire template (dislocation density of $\sim 10^9$ cm^{-2}) from Kyma. Both N-polar and Ga-polar templates were cleaved into $\sim 1 \times 1$ cm^2 sized pieces and coloaded on a single silicon wafer using indium bonding to ensure identical growth conditions. This was to make sure that the difference in In incorporation for $In_xGa_{1-x}N$ of both polarities at a particular growth temperature could be studied. Since sapphire has a lower thermal conductivity than GaN, the surface temperature (using optical pyrometer) of the Ga-polar sample was found to be 3–5 °C higher than that of the N-polar sample. All InGaN layers discussed in this work were grown for 1 h with a standard GaN growth rate of 5 nm/min. However, due to decomposition of InGaN, the actual thickness of the films is expected to be less than expected from the nominal growth rate (i.e., 300 nm).

Three sets of growths were done at growth temperatures of 500, 550, and 600 °C in an In-rich regime, the temperatures being stabilized prior to growth. The growth temperature was monitored by an optical pyrometer with readings calibrated against the melting point of Al. The In incorporation depends on the growth temperature and on the Ga/N-flux ratio;[7] the Ga flux was kept constant at 9.5×10^{-8} Torr which corresponds to ~0.39 times the stoichiometric GaN growth rate. A rf power of 350 W and N_2 flow rate equivalent to 1.9×10^{-5} Torr of beam flux monitor pressure corresponding to a stoichiometric growth rate of 5 nm/min were used throughout. All growths were done in In-rich regime with an In flux of 5×10^{-7} Torr which is more than twice the stoichiometric Ga flux. We have assumed a "strong stoichiometric condition"[15] which refers to the assumption that all impinging Ga atoms would be incorporated into the lattice and only those sites which have not been Ga occupied would be available for In incorporation. This translates into the fact that a variation in In incorporation is simply dependent on growth temperature and Ga flux in a N-limited growth regime.

Light emission from the N-polar and Ga-polar InGaN samples was collected by 1-m-long monochromator with a ruled grating of 1200 g/mm placed at surface normal and the signals were detected by Hamamatsu R2658 photomultiplier tube mounted exit slit of the monochromator. A Stanford Research System SR830 DSP lock-in amplifier was used to analyze the data. Ar ion laser with a wavelength of 488 nm was used as an excitation light source. The photoluminescence (PL) excitation density is 276 mW cm^{-2}. A control sample was used to confirm that the measurements were performed in identical conditions so that PL intensity values between each measurement performed can be comparable. All measurements were done at room temperature. Triple axis ω-2θ x-ray diffraction (XRD) scans of the samples were performed symmetric around on-axis (0002) and (000$\bar{2}$) for Ga polar and N polar, respectively, using a Bede high resolution XRD system with Cu $K\alpha_1$ radiation (k=1.540 56 Å) and a Ge hybrid monochromator. The atomic force microscope (AFM) scans were performed using a Veeco DI 3000 AFM equipment in tapping mode configuration.

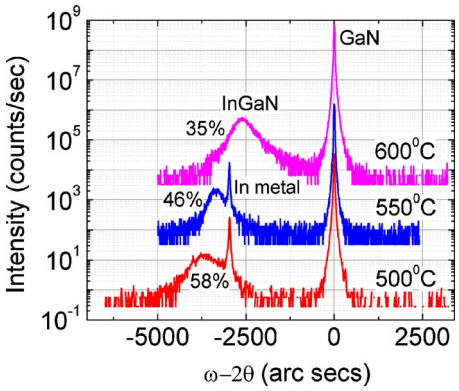

FIG. 1. (Color online) High resolution XRD ω-2θ triple-axis scans of the N-polar InGaN films showing no phase segregation or compositional nonuniformity.

III. RESULTS

Figure 1 shows the ω-2θ triple-axis scans of the N-polar films. All N-polar samples showed a single InGaN peak indicating the absence of phase segregation or compositional nonuniformity in the range of compositions (0%–58%) explored here. Using the growth model (derived later in this work), the thicknesses of all N-polar and Ga-polar $In_xGa_{1-x}N$ films are at least 150 nm. Since this is much higher than the critical thickness[17,18] corresponding to the relaxation of $In_xGa_{1-x}N$ on GaN for compositions obtained in this study, we can safely assume all the films to be fully relaxed. The In compositions for the N-polar $In_xGa_{1-x}N$ films as extracted from XRD data assuming complete relaxation are indicated beside each plot (Fig. 1).

In Fig. 2, the variation of the In compositions of the $In_xGa_{1-x}N$ films of both polarities as obtained from room temperature PL peaks and XRD scans as a function of growth temperature is shown. The energy band-gap values extracted from the room temperature PL peaks were used to determine the In compositions in the films using bowing parameter of b=1.8 eV from Ref. 19 with a GaN band gap =3.4 eV. The wavelength corresponding to the lowest composition Ga-polar InGaN (~14% from XRD) grown at 600 °C was outside the range of the PL setup since its emission wavelength is expected to be lower than the excitation light source wavelength (488 nm, >2.541 eV). The compositions determined from PL measurements are close to those obtained from XRD scans using linear interpolation of lattice constants (Vegard's law). The small mismatch between the

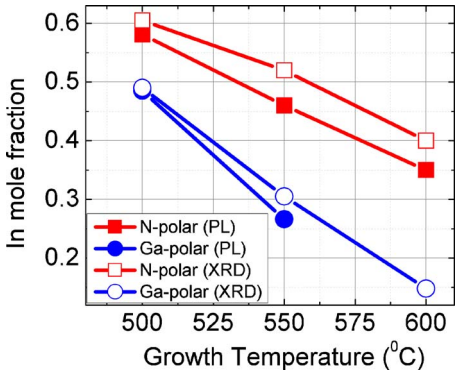

FIG. 2. (Color online) Indium mole fraction as a function of growth temperature for both Ga and N-polar InGaN films as extracted from room temperature PL peaks and XRD scans.

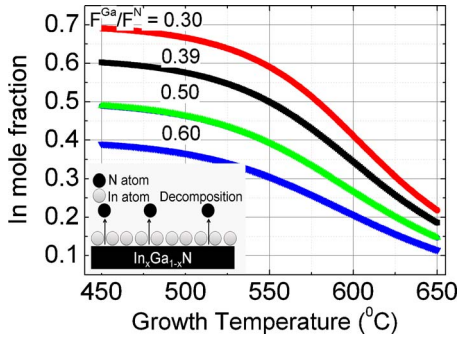

FIG. 3. (Color online) Indium mole fraction as a function of growth temperature for various Ga/N-flux ratios as predicted by our growth model for N-polar $In_xGa_{1-x}N$.

two ways of composition estimation can be attributed to uncertainty in bowing parameter as well as to the nonideality of Vegard's law. Also for PL, the energy band gaps have been extracted from room temperature PL peak positions and related these to the In content. The PL peak position, however, cannot be related precisely to the band gap. Because of the typical higher energy of the PL peak positions with respect to the actual band gap, this may cause decreased In contents as derived from PL. From Fig. 2, it is clear that In incorporation drops as growth temperature increases due to higher decomposition of InN at higher temperatures irrespective of the polarity. Besides, for a given growth temperature, In incorporation is higher for N-polar $In_xGa_{1-x}N$ than for Ga-polar $In_xGa_{1-x}N$. This implies that N-polar $In_xGa_{1-x}N$ can be grown at a higher temperature for a specified In-mole fraction than Ga-polar $In_xGa_{1-x}N$.

IV. DISCUSSION

We developed[20] a growth model for N-polar $In_xGa_{1-x}N$ based on InN decomposition to explain the growth temperature and Ga-flux dependent compositional variation of In-mole fraction and later extend it for Ga-polar $In_xGa_{1-x}N$ as well. The model has been developed for the metal rich N-limited growth regime where the active N flux available determines the nominal growth rate with an excess of In coverage on the surface. Thus, the composition of In in $In_xGa_{1-x}N$ samples is independent of In atoms impinging on or desorbing from the surface. It has been shown[11] that N-polar InN decomposition in the metal rich growth regime can be considered to be N atoms leaving the surface (inset of Fig. 3). If F^N is the nitrogen-stoichiometric flux defining the growth rate in the absence of decomposition, then the actual stoichiometric flux F^{N^*} defining the true growth rate as InN decomposes is less than F^N by a decomposition rate F^D,

$$F^{N^*} = F^N - F^D \tag{1}$$

The In composition, x, in an $In_xGa_{1-x}N$ film is related to the effective (reduced) growth rate F^{N*} and the incident Ga flux, F_{Ga}, by the equation (assuming strong stoichiometric condition[15])

$$x = 1 - \frac{F^{Ga}}{F^{N^*}}. \tag{2}$$

We assume that the decomposition rate F^D is proportional to the In-mole fraction x in the $In_xGa_{1-x}N$ film (so that for a pure GaN film, there will be no decomposition as expected). The decomposition rate F^D is also shown to have an Arrhenius dependence on substrate temperature T_{sub},[11]

$$F^D \propto x \exp\left(-\frac{E_a}{kT}\right), \tag{3}$$

where E_a is the activation energy of decomposition of N-polar InN which has been calculated earlier to be 1.2 eV.[11] Using Eqs. (1) and (4) in Eq. (3), the In-composition x in the $In_xGa_{1-x}N$ film can be expressed as a function of temperature,

$$x = \frac{(1+\beta e^{(-E_a/kT)}) - \sqrt{(1+\beta e^{(-E_a/kT)})^2 - 4\beta e^{(-E_a/kT)}(1 - F^{Ga}/F^N)}}{2\beta e^{(-E_a/kT)}}, \tag{4}$$

where β is the proportionality factor of Eq. (3) normalized to the value of nitrogen flux.

The activation energy E_a=1.2 eV obtained in Ref. 11 is in the temperature range of 590–635 °C and so using this

value of E_a might not be accurate for a temperature range of 450–650 °C modeled in our study. It has been pointed out that[16] In loss cannot be accounted for simply by a single thermally activated process since the surface stoichiometric modifies the process behind it, implying a temperature dependence of E_a. However, the exact dependence of E_a for InN decomposition on growth temperature is not yet well understood or derived and hence we shall use the value reported in Ref. 11 for our work here with a room for better accuracy provided we know E_a as a function of temperature. It is also noteworthy that in Ref. 14, the activation energy for $In_xGa_{1-x}N$ decomposition is reported to be 3.5 eV as extracted from the plot of the ratio of InN loss to In composition vs $1/kT$. However, a value of activation energy of $In_xGa_{1-x}N$ decomposition reported in Ref. 14 would require a revision now in the light of a revised and correct InN band gap of ~0.7 eV. From the data points obtained in this study, we plotted the ratio of F^D/x^{In} vs $1/kT$ (not shown here) and from the slope, derived $E_a \sim 1.5$ eV which is close to 1.2 eV reported in Ref. 11. The difference springs from various factors such as dependence of E_a on growth temperature, value of 1.2 eV (Ref. 11) reported for 590–635 °C range, and uncertainty in precisely determining the In composition (from both PL and XRD).

Using Eq. (4) and the data points of In composition corresponding to the three N-polar $In_xGa_{1-x}N$ samples, a curve fitting was done to evaluate β. The resulting variation in x as a function of substrate temperature as obtained from our model is plotted in Fig. 3. The different curves correspond to different Ga/N-flux ratios. As can be observed, In incorporation x decreases as Ga/N-flux ratio increases for a given growth temperature. Thus, using the curves as guidelines, a required In composition x can be achieved either by choosing the growth temperature and determining the Ga/N-flux ratio from the plots or vice versa. This growth model thus provides comprehensive flexibility in obtaining higher In incorporation even at higher growth temperatures by choosing the required Ga/N-flux ratio.

To validate our growth model, we plotted the experimentally obtained data points (i.e., In composition x) for N-polar $In_xGa_{1-x}N$ for a Ga/N-flux ratio of 0.39 used in this work. As shown in Fig. 4, the data points are found to be in good agreement with the curve predicted by our growth model. Besides, using the same approach as used for N-polar $In_xGa_{1-x}N$, we use the same set of equations for modeling the growth of Ga-polar $In_xGa_{1-x}N$. The E_a for decomposition of In-polar InN, however, has been investigated earlier for lower growth temperatures only (<500 °C) and found to be 1.92 eV.[21] The prefactor relating the decomposition rate to growth temperature and In-mole fraction [Eq. (3)] is expected to be the same for growth kinetics of both Ga-polar and N-polar $In_xGa_{1-x}N$ since it accounts for any factor which is not temperature dependent. More precisely, the prefactor is related to the number of planar sites containing N atoms on the surface because that is what is assumed to define the decomposition of InN apart from temperature and In-mole fraction. In simple words, with a different prefactor for Ga-polar polarity, the higher incorporation of In in N-polar $In_xGa_{1-x}N$ at the same growth temperature can no longer be attributed to a difference in E_a only. Borrowing the value of prefactor from the growth model developed for N-polar polarity of $In_xGa_{1-x}N$, we use a Ga/N-flux ratio of 0.39 used in this work with E_a as the unknown while fitting the data points for Ga-polar $In_xGa_{1-x}N$. The activation energy for Ga-polar polarity is thus found to be 1.12 eV against 1.2 eV for N-polar polarity. Again, the data points are found to be in nice fit with the model as shown in Fig. 4. Several data points showing In compositions and growth temperatures for Ga-polar $In_xGa_{1-x}N$ by PAMBE from the literature[4,22–24] have also been included in Fig. 4 as a comparison. The higher In incorporation for N-polar polarity is obvious from Fig. 4.

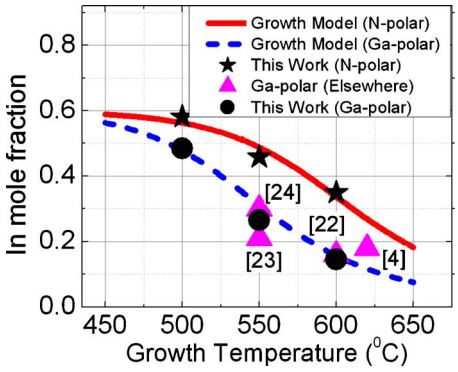

FIG. 4. (Color online) Experimental data points obtained in this work fitted to curves predicted by our growth model for both N-polar and Ga-polar polarity $In_xGa_{1-x}N$; a few data points from reports published elsewhere are also shown to stress the overall higher achievability of indium incorporation in N-polar polarity. Inset: schematic of InN decomposition modeled as nitrogen atoms leaving the surface.

The decomposition rate can be quantitatively estimated as $F^D \infty x \exp[-(E_a/kT)]$, and therefore the reduced growth rate $F^{N^*} = F^N - F^D$ as a function of growth temperature. Figure 5 shows the overall growth diagram for N-polar $In_xGa_{1-x}N$ growth by MBE calculated using experimental composition and temperature values from this study. The stoichiometric growth rate in the absence of decomposition is 5 nm/min; to

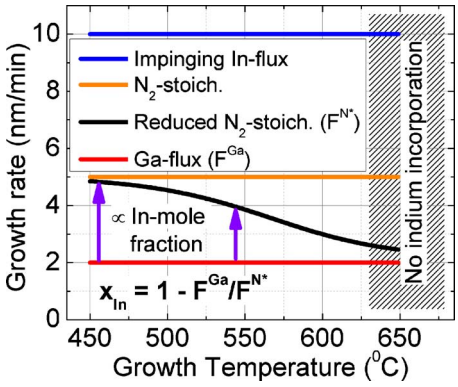

FIG. 5. (Color online) Growth diagram for the growth of N-polar $In_xGa_{1-x}N$: the difference between reduced nitrogen stoichiometric and Ga flux defines indium incorporation assuming strong stoichiometric condition.

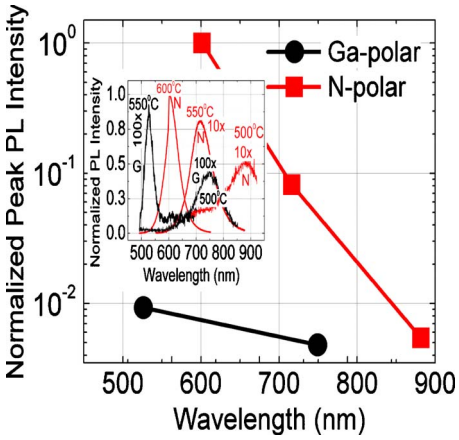

FIG. 6. (Color online) Peak PL intensity (normalized with respect to the highest intensity obtained) and full width at half maximum of InGaN samples of both polarities as a function of wavelengths (corresponding to band gaps extracted from room temperature PL measurements). The lines are a guide for the eyes. Inset: PL intensity (normalized with respect to the highest intensity obtained) of Ga-polar and N-polar InGaN on a linear scale; the magnification factor, polarity (**G** for Ga polar and **N** for N polar), and growth temperature are indicated against each peak.

ensure excess In coverage, an In flux of approximately twice the stoichiometric (~10 nm/min) is used while the Ga flux used is ~2 nm/min which is 0.4 times the usual growth rate of 5 nm/min. As seen, in the presence of decomposition, the growth rate no longer stays constant at 5 nm/min but drops significantly with increasing growth temperature. The difference between the reduced nitrogen stoichiometric (or reduced growth rate) and the Ga flux, i.e., $F^{N*}-F^{Ga}$, in fact, corresponds to the amount of In incorporated. Thus, from Fig. 5, the decreasing In incorporation for a given Ga/N-flux ratio with increasing growth temperature becomes clear.

The model developed above is valid in temperature and In-flux regimes where a stable excess indium coverage is maintained. It has been established[11] that in PAMBE growth of N-polar InN, metallic In accumulation (adlayer and droplets) on the surface due to In flux from InN decomposition and impinging In atoms from the source is limited by maximum In-desorption rate F^{des} up to a growth temperature of ~610 °C.[11] However, at higher growth temperatures above ~610 °C, desorption rate of In exceeds decomposition rate of InN. In Fig. 5, the shaded region above ~630 °C has been indicated to have "no indium incorporation" as excess In can remain on the surface in the form of droplets only if the impinging In flux is greater than $|F^{des}-F^{D}|$. If the surface is devoid of excess In but there is an excess of N, the growth will shift to In-limited regime instead of being N limited thus invalidating our growth model. Since all our growths have been performed in an In-rich regime at temperatures below ~610 °C, the In incorporation will depend only on the reduced N-flux F^{N^*} and the Ga-flux F^{Ga} which remains unchanged.

To assess the optical quality of the N-polar InGaN films, we plot the PL intensity for the various N-polar and Ga-polar $In_xGa_{1-x}N$ samples in a linear scale (inset of Fig. 6) with the intensities of Ga-polar samples multiplied 100 times to bring them to a comparable level to the peak intensity of the N-polar sample grown at 600 °C corresponding to 600 nm emission. The intensities of other N-polar InGaN samples are multiplied ten times as well. Figure 6 shows on its left axis the peak intensity corresponding to the PL measurements of each sample against the corresponding wavelength. The peak intensity for N-polar $In_xGa_{1-x}N$ samples shows more than two orders of magnitude increase as wavelength decreases from ~900 to ~600 nm, corresponding to a 100 °C increase in growth temperature. Besides, the N-polar sample shows much higher intensity than the Ga-polar sample especially at shorter wavelengths. However, the surface roughness or morphological difference plays a major role in PL intensity. Figure 7 shows the (5×5 μm^2) AFM scans of both Ga-polar and N-polar samples grown at 550 and 600 °C. As can be seen, the N-polar samples have relatively higher rms roughness than that of the Ga-polar samples. Particularly, the N-polar sample grown at 600 °C has a very high rms roughness of ~15 nm. The surface morphologies of a particular sample were found to be similar in various regions of the sample concerned. This might explain the relatively higher PL intensity of N-polar (bulk) InGaN samples. Besides, the composition of In in the Ga-polar and N-polar samples grown at a particular temperature is different, and hence it would not be justified to comment on the optical qualities of the samples containing different In compositions.

To investigate the surface morphology of InGaN multiple quantum well (MQW) grown under these conditions, a test sample was grown at ~625 °C in identical conditions as for the growth of the multiple quantum-well structure (explained later) with a single ~3-nm-thick $In_{0.31}Ga_{0.69}N$ layer covered by ~2 nm of $In_{0.05}Ga_{0.95}N$ barrier to prevent the decomposition of the active layer as the sample was cooled down. The surface was found to be smooth with rms roughness of ~0.5 nm for a 2×2 μm^2 AFM scan (inset of Fig. 8).

Based on our growth model, a Ga/N-flux ratio was chosen to achieve 29% In-mole fraction in an $In_xGa_{1-x}N/GaN$ MQW structure corresponding to green (~520 nm) emission. Figure 8 shows the epitaxial structure grown. The growth temperature for the growth of active regions was chosen to be ~625–630 °C which is fairly high for PAMBE growth of $In_xGa_{1-x}N$ in general. The growth of $In_xGa_{1-x}N$ and GaN successively for MQW without growth interruption with only one Ga source poses severe challenges. Both the optimal growth temperature and the Ga flux for the growth of $In_xGa_{1-x}N$ and GaN are significantly different. A pulsing scheme was employed to grow the GaN barrier: the In and Ga shutters were open throughout the barrier growth while the nitrogen shutter was pulsed with a duty cycle equal to the Ga/N-flux ratio, the Ga-flux being the same as used in the preceding $In_xGa_{1-x}N$ quantum-well layer. Using our growth model, the decomposition rate was calculated for the given growth conditions to determine the actual growth time to achieve 3-nm-thick quantum wells. A fitting of the dynamic simulation of triple-axis ω-2θ HRXRD scan with the actual scan data (inset of Fig. 8) indicated a close match of the In composition and thickness to that originally aimed for thus

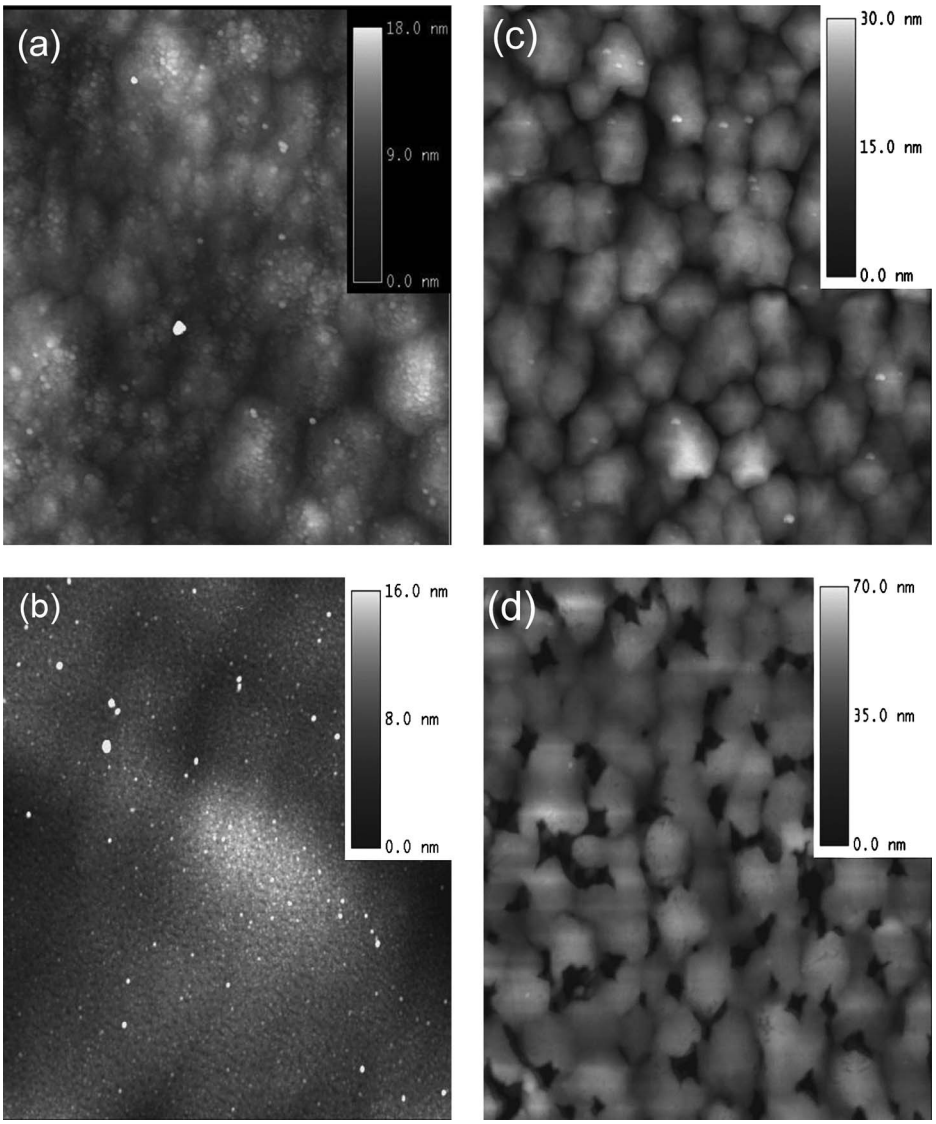

FIG. 7. AFM scans of (5×5 μm^2) $In_xGa_{1-x}N$ films: (a) Ga polar, 550 °C, rms ~ 2.8 nm; (b) Ga polar, 600 °C, rms ~ 2.3 nm; (c) N polar, 550 °C, rms ~ 5.7 nm; and (d) N polar, 600 °C, rms ~ 14.1 nm.

once again validating our growth model. Postgrowth 3×3 reconstructions were observed while sample was cooled indicating N-polar polarity; the top p^+ GaN layer was found to have smooth surface morphology (AFMs not shown)

In conclusion, a comprehensive growth model for the growth of N-polar $In_xGa_{1-x}N$ by PAMBE has been proposed and validated which explains quantitatively the variation of In incorporation as a function of growth temperature and Ga/N-flux ratio. It has been extended for Ga-polar $In_xGa_{1-x}N$ as well and found to fit experimental data points excellently. The model has been found to predict In incorporation x in N-polar $In_xGa_{1-x}N$ grown under different growth (i.e., various growth temperatures and Ga fluxes) conditions fairly accurately. Finally, an $In_{0.31}Ga_{0.69}N/In_{0.05}Ga_{0.95}N$ MQW structure was grown with conditions predicted by our growth model. Our growth model is hence expected to guide the growth of N-polar $In_xGa_{1-x}N$ by PAMBE in a wide range of growth conditions for optoelectronic device applications.

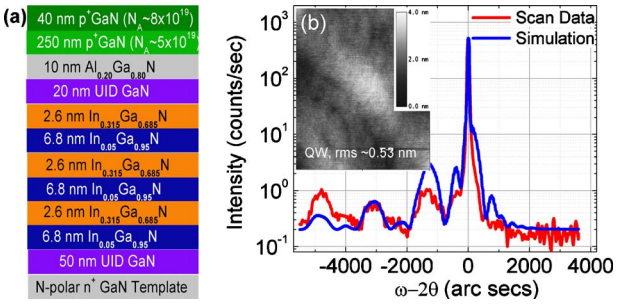

FIG. 8. (Color online) (a) Epitaxial structure used for InGaN/GaN MQW; (b) XRD scan data and simulation confirming the composition and thicknesses of epilayers; Inset: AFM of the quantum well (with two barriers) showing smooth surface.

ACKNOWLEDGMENTS

The authors would like to acknowledge funding from ONR (Program manager: Paul Maki) and OSU Institute for Materials Research (IMR). E.G. would like to thank The Scientific and Technological Research Council of Turkey (TUBITAK) Grant No. 2219 project program for the support.

[1]C. J. Neufeld, N. G. Toledo, S. C. Cruz, M. Iza, S. P. DenBaars, and U. K. Mishra, Appl. Phys. Lett. **93**, 143502 (2008).
[2]B. Heying, R. Averbeck, L. F. Chen, E. Haus, H. Riechert, and J. S. Speck, J. Appl. Phys. **88**, 1855 (2000).
[3]T. Ive, O. Brandt, M. Ramsteiner, M. Giehler, H. Kostial, and K. H. Ploog, Appl. Phys. Lett. **84**, 1671 (2004).
[4]C. Thomidis, A. Yu. Nikiforov, T. Xu, and T. D. Moustakas, Phys. Status Solidi C **5**, 2309 (2008).
[5]M. Siekacz *et al.*, Phys. Status Solidi C **6**, S917 (2009).
[6]S. Rajan, A. Chini, M. H. Wong, J. S. Speck, and U. M. Mishra, J. Appl. Phys. **102**, 044501 (2007).
[7]M. H. Wong, Ph.D. thesis, UCSB, 2009.
[8]K. Xu and A. Yoshikawa, Appl. Phys. Lett. **83**, 251 (2003).
[9]H. Naoi, F. Matsuda, T. Araki, A. Suzuki, and Y. Nanishi, J. Cryst. Growth **269**, 155 (2004).
[10]G. Koblmüller, C. S. Gallinat, S. Bernardis, J. S. Speck, G. D. Chern, E. D. Readinger, H. Shen, and M. Wraback, Appl. Phys. Lett. **89**, 071902 (2006).
[11]G. Koblmüller, C. S. Gallinat, and J. S. Speck, J. Appl. Phys. **101**, 083516 (2007).
[12]J. Abell, Ph.D. thesis, Boston University, 2008.
[13]S. Keller, N. A. Fichtenbaum, M. Furukawa, J. S. Speck, S. P. DenBaars, and U. K. Mishra, Appl. Phys. Lett. **90**, 191908 (2007).
[14]R. Averbeck and H. Riechert, Phys. Status Solidi A **176**, 301 (1999).
[15]D. F. Storm, J. Appl. Phys. **89**, 2452 (2001).
[16]M. L. O'Steen, F. Fedler, and R. J. Hauenstein, Appl. Phys. Lett. **75**, 15 (1999).
[17]D. Holec, P. M. F. J. Costa, M. J. Kappers, and C. J. Humphreys, J. Cryst. Growth **303** (2007).
[18]C. A. Parker, J. C. Roberts, S. M. Bedair, M. J. Reed, S. X. Liu, and N. A. El-Masry, Appl. Phys. Lett. **75**, 2776 (1999).
[19]M. Kurouchi, T. Araki, H. Naoi, T. Yamaguchi, A. Suzuki, and Y. Nanishi, Phys. Status Solidi B **241**, 2843 (2004).
[20]D. N. Nath, E. Gur, S. A. Ringel, and S. Rajan, Appl. Phys. Lett. **97**, 071903 (2010).
[21]C. S. Gallinat, G. Koblmüller, J. S. Brown, and J. S. Speck, J. Appl. Phys. **102**, 064907 (2007).
[22]X. Q. Shen, T. Ide, M. Shimizu, and H. Okumura, J. Cryst. Growth **237–239**, 2 (2002).
[23]Y. E. Romanyuk, L. D. Kranz, and S. R. Leone, J. Appl. Phys. **103**, 073104 (2008).
[24]X. Chen, K. D. Matthews, D. Hao, W. J. Schaff, and L. F. Eastman, Phys. Status Solidi A **205**, 5 (2008).